Periodic Trends in Reactions of Benzene Clusters of Transition Metal Cations, M(C 6 H 6) 1,2 + , with Molecular Oxygen †

ARTICLE *in* THE JOURNAL OF PHYSICAL CHEMISTRY A · OCTOBER 2002

Impact Factor: 2.69 · DOI: 10.1021/jp0208900

Periodic Trends in Reactions of Benzene Clusters of Transition Metal Cations, $M(C_6H_6)_{1,2}^+$, with Molecular Oxygen†

Doina Caraiman and Diethard K. Bohme*

Department of Chemistry, Centre for Research in Mass Spectrometry, and Centre for Research in Earth and Space Science, York University, Toronto, Ontario M3J 1P3, Canada

Received: April 3, 2002; In Final Form: June 27, 2002

Mono- and bis-adducts of benzene of the type $M(C_6H_6)_{1,2}^+$ have been generated in the gas phase with first-, second-, and third-row transition metal cations, and their reactivities toward molecular oxygen have been measured using an inductively coupled plasma/selected-ion flow tube (ICP/SIFT) tandem mass spectrometer. Trends in reactivity were identified for the metal cation adducts across and down the periodic table. The intrinsic effect of the benzene ligand(s) on the reactivity of the bare metal cations was determined through comparisons with earlier results obtained for the bare metal ions. Molecular oxygen activation by early transition metal cations is preserved in the presence of one benzene ligand but almost disappears in the presence of two benzene molecules. The rate coefficients for O_2 addition to late transition metal−benzene adducts are enhanced by up to 4 orders of magnitude in the presence of benzene. Thermochemical information is derived from the occurrence or absence of ligand-switching or metal-abstraction reactions. Oxidation of the benzene ligand itself was observed to be mediated by the transition metal cations V^+, Cr^+, Fe^+, Co^+, and Re^+ and appeared to result from simultaneous activation of C−H, C−C, and O−O bonds. Catalytic oxidation of the benzene ring observed in the presence of Fe^+, Cr^+, and Co^+ is postulated to result in the production of catechol.

Introduction

The study of the chemistry of transition metals in the gas phase is an active area of research; transition metals play a critical role in a variety of chemistries ranging from industrial catalysis to biological activity. It is therefore important to understand the fundamental aspects of the intrinsic chemistry of transition metals. Bare metal cations can be generated in the gas phase and their intrinsic chemistry can be explored using techniques of mass spectrometry.[1] Modern mass-spectrometric techniques allow for the gas-phase study of the chemistry of more complex metal-cation-containing species with compositions and structures that resemble "real-life" situations more closely. For example, the effects of ligation on the bare metal cation reactivity can be assessed, with the results providing a benchmark for similar effects in condensed-phase chemistry.[2a−i]

Large biological molecules can not easily be accessed directly for mass spectrometric studies because of low vapor pressure and/or thermal instability. However, the metal cation binding site of a large molecule can be simulated in a small volatile and stable molecule with the appropriate structure. For example, metal cation π interactions in biological systems can be "mimicked" by adducts of metal cations and benzene. Benzene is readily introduced intact into mass spectrometers as a vapor. Indeed, benzene has become a prototype aromatic molecule in the study of the cation π interactions that determine the structures of biomolecules.[3a−c]

The interactions of metal cation−benzene adducts with molecular oxygen can be used to model the oxidation of larger biological systems. Transition metal cations are usually the active sites in such processes and mediate oxidation reactions by binding molecular oxygen reversibly (O_2 transport by myoglobin) or by delivering an O-atom to various substrates (cytochrome P-450).[4] Also, there is increasing interest in the role of metal ion interactions with benzene in interstellar chemistry in which benzene can contribute to the depletion of atomic ions and can act as a platform for catalytic gas-phase chemistry.[5a−c]

The present work investigates ion−molecule reactions of transition metal cation−benzene clusters with molecular oxygen in the gas phase. The influence of one and two benzene ligands on the "bare" metal cation reactivity is assessed through a comparison with results obtained in the absence of benzene that were presented previously.[6] Periodic trends in reactivity are explored for both $MC_6H_6^+$ and $M(C_6H_6)_2^+$ reacting with O_2.

The oxidation of the benzene substrate mediated by the metal cations is also investigated. Oxidation is an important route to the degradation of carcinogenic benzene with relevance to human health and environmental contamination.[7a,b] Also, the oxidation of benzene to phenol has industrial importance.[8] These processes usually require the presence of a catalyst. We investigate here the use of transition metal cations as promoters for such processes in the gas phase. Transition metal cations are known to activate the C−C, C−H, and O−O bonds in specific gas-phase reactions.[9a−c]

Experimental Section

The kinetic results reported here were obtained using a selected-ion flow tube (SIFT) tandem mass spectrometer. The experimental setup and operating conditions for the SIFT apparatus have been described in detail previously.[10a,b] All measurements were performed in a helium buffer gas with a pressure of 0.35 ± 0.01 Torr. The metal ions were generated in an inductively coupled plasma (ICP) source interfaced with the SIFT instrument. Detailed descriptions of the ICP ion source

† Part of the special issue "Jack Beauchamp Festschrift".

* Corresponding author. E-mail dkbohme@yorku.ca; phone 416-736-2100, ext 66188; fax 416-736-5936.

10.1021/jp0208900 CCC: $22.00
Published on Web 09/12/2002

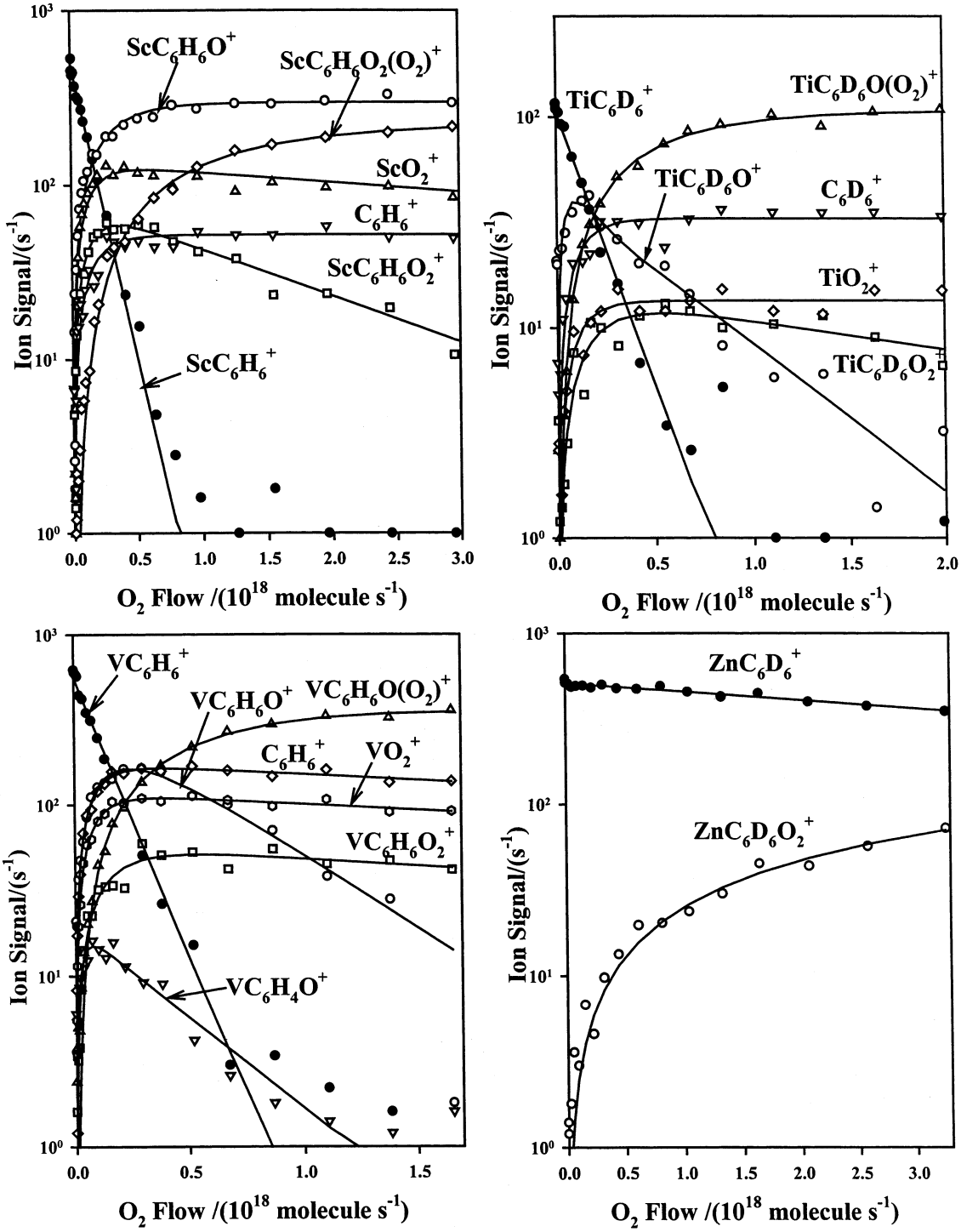

Figure 1. Composite of ICP/SIFT results for the reactions of the first-row transition metal ion−benzene monoadducts $ScC_6H_6^+$, $TiC_6D_6^+$, $VC_6H_6^+$, and $ZnC_6D_6^+$ with O_2 in helium buffer gas at 0.35 ± 0.01 Torr and 295 ± 2 K.

and interface as well as the plasma conditions[11] and the state distribution for the transition metal ions generated[6] have been provided previously.

The metal ions were mass-selected with the quadrupole mass filter and injected into the flow tube containing He buffer gas. Vaporized benzene (or deuterated benzene) was introduced upstream in the flow tube through a leak valve. The reactions of most metal cations with benzene generate adducts, usually with up to two molecules of benzene clustering at the metal cation.[12] The flow of benzene vapor was optimized so that the intensity of the benzene adduct of interest [$MC_6H_6^+$ or $M(C_6H_6)_2^+$] predominated over the intensities of other ions present. The typical flow of benzene in the flow tube was approximately 4×10^{16} molecule s^{-1} for optimum $MC_6H_6^+$ formation and 5×10^{17} molecule s^{-1} for optimum $M(C_6H_6)_2^+$ formation. Such flow rates are comparable to the flow of oxygen used in the kinetic measurements, which ranges from 0 to 5×10^{18} molecule s^{-1}.

The ions are thermalized by collisions with He buffer gas (about 10^5 collisions) before entering the reaction region downstream in the flow tube where the oxygen is added as a neutral reagent. The collisions with He ensure that the reactant ions reach a translational temperature equal to the tube temperature of 295 ± 2 K prior to the reaction.

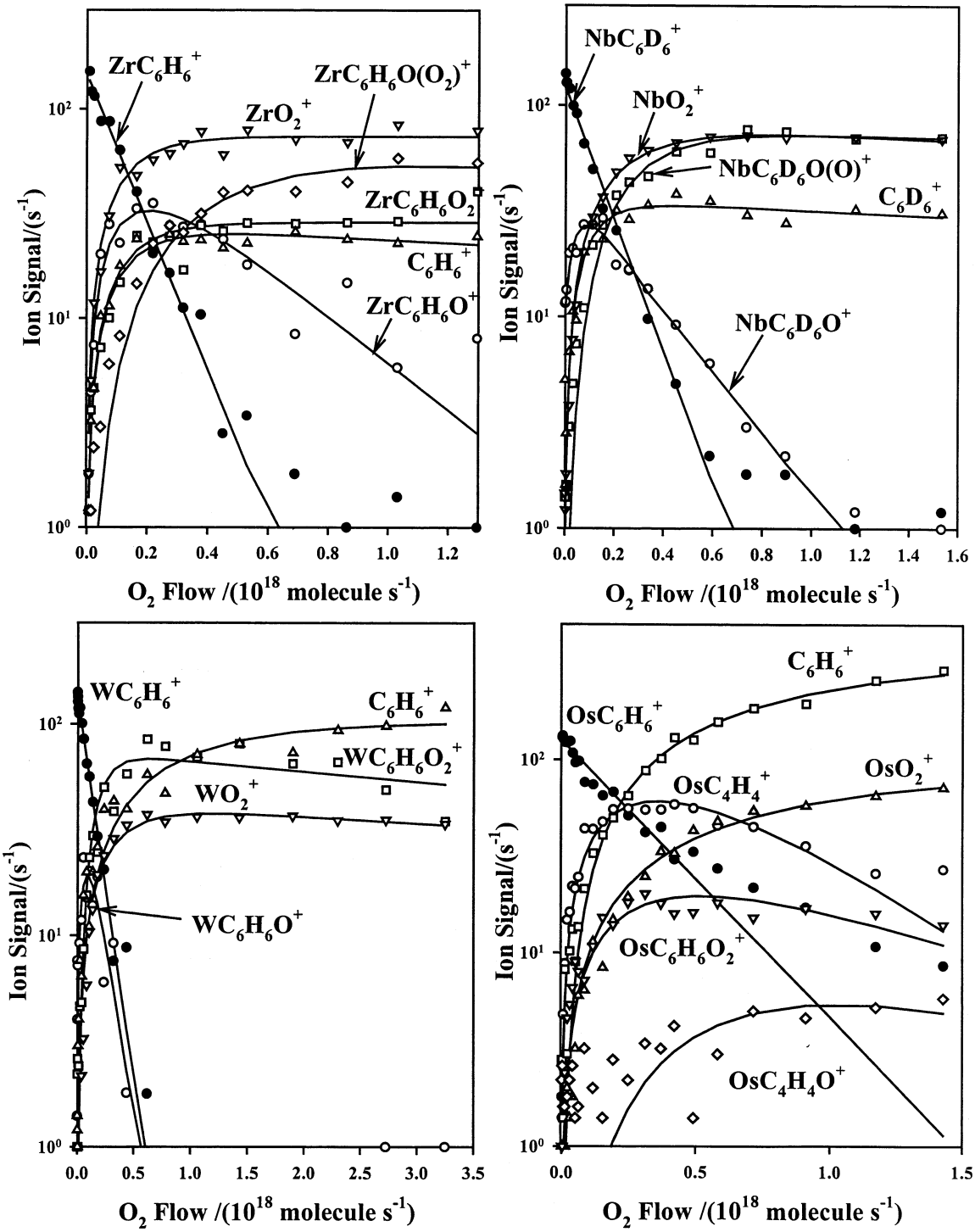

Figure 2. Composite of ICP/SIFT results for the reactions of the selected second and third-row transition metal ion−benzene monoadducts $ZrC_6H_6^+$, $NbC_6D_6^+$, $WC_6H_6^+$, and $OsC_6H_6^+$ with O_2 in helium buffer gas at 0.35 ± 0.01 Torr and 295 ± 2 K.

Reactant and product ions are monitored still further downstream with a second quadrupole mass filter as a function of the neutral reagent flow. Rate coefficients for the primary reactions of all ions present in the system are determined with an uncertainty of ±30% from the rate of decay of the reactant ion intensity using pseudo-first-order kinetics. Higher-order rate coefficients are obtained by fitting the experimental data to the solutions of the system of differential equations for a chain of successive reactions.

The multicollision-induced dissociation (CID) of sampled ions is investigated by raising the potential of the sampling nose cone from 0 to −80 V.[13] Thresholds for dissociation are obtained from plots of relative ion intensities as a function of accelerating voltage, and the results provide insight into bond connectivities.

Benzene (>99.0%) or deuterated benzene-d_6 (≥99.6% D) was used without further purification except for multiple freeze−pump−thaw cycles to remove noncondensable gases. Ultra-high-purity (99.98%) oxygen was introduced into the reaction region as a mixture in helium (10−20%).

Results and Discussion

Overview. All of the first-, second-, and third-row transition metal cations, except Tc^+ because of its radioactivity, were

TABLE 1: Reaction Rate Coefficients (k_{obs} in cm^3 molecule^{-1} s^{-1}) for Primary Reactions of Transition Metal Cations, M^+, and Benzene Adducts of Transition Metal Cations, $MC_6H_6^+$ and $M(C_6H_6)_2^+$, with O_2 in He at 0.35 ± 0.01 Torr and 295 ± 2 K

M	M^+	$MC_6H_6^+$	$M(C_6H_6)_2^+$	M	M^+	$MC_6H_6^+$	$M(C_6H_6)_2^+$	M	M^+	$MC_6H_6^+$	$M(C_6H_6)_2^+$
Sc	3.7×10^{-10}	4.0×10^{-10}	4.4×10^{-11}	Y	4.7×10^{-10}	3.8×10^{-10}	1.8×10^{-10}	La	4.3×10^{-10}	4.4×10^{-10}	3.4×10^{-10}
Ti	4.7×10^{-10}	3.3×10^{-10}	$<1.0 \times 10^{-14}$	Zr	5.0×10^{-10}	4.3×10^{-10}	6.2×10^{-11}	Hf	4.1×10^{-10}	3.5×10^{-10}	1.6×10^{-11}
V	3.0×10^{-10}	4.2×10^{-10}	$<1.0 \times 10^{-14}$	Nb	5.0×10^{-10}	4.0×10^{-10}	5.4×10^{-12}	Ta	4.6×10^{-10}	3.5×10^{-10}	1.7×10^{-12}
Cr	2.2×10^{-13}	$\geq 1.3 \times 10^{-10}$	$<1.0 \times 10^{-14}$	Mo	7.5×10^{-11}	2.6×10^{-10}	$<1.0 \times 10^{-14}$	W	4.0×10^{-10}	3.7×10^{-10}	$<1.0 \times 10^{-14}$
Mn	$<1.0 \times 10^{-14}$	$\geq 4.5 \times 10^{-11}$	$<1.0 \times 10^{-14}$	Tc	NA[a]	NA[a]	NA[a]	Re	1.1×10^{-12}	$\geq 1.5 \times 10^{-10}$	$<1.0 \times 10^{-14}$
Fe	4.3×10^{-13}	$\geq 1.8 \times 10^{-10}$	$<1.0 \times 10^{-14}$	Ru	1.6×10^{-13}	$\geq 1.8 \times 10^{-10}$	$<1.0 \times 10^{-14}$	Os	1.6×10^{-12}	$\geq 1.9 \times 10^{-10}$	$<1.0 \times 10^{-14}$
Co	1.5×10^{-13}	$\geq 1.0 \times 10^{-10}$	$<1.0 \times 10^{-14}$	Rh	1.9×10^{-14}	$\geq 1.1 \times 10^{-10}$	$<1.0 \times 10^{-14}$	Ir	7.1×10^{-14}	$\geq 1.5 \times 10^{-10}$	$<1.0 \times 10^{-14}$
Ni	5.0×10^{-14}	$\geq 6.4 \times 10^{-11}$	$<1.0 \times 10^{-14}$	Pd	1.5×10^{-14}	$\geq 5.4 \times 10^{-12}$	$<1.0 \times 10^{-14}$	Pt	1.0×10^{-14}	$\geq 1.1 \times 10^{-10}$	$<1.0 \times 10^{-14}$
Cu	2.6×10^{-13}	$\geq 6.6 \times 10^{-13}$	$<1.0 \times 10^{-14}$	Ag	4.5×10^{-13}	$<1.6 \times 10^{-12}$	$<1.0 \times 10^{-14}$	Au	1.4×10^{-13}	$\geq 2.1 \times 10^{-12}$	$<1.0 \times 10^{-14}$
Zn	2.7×10^{-13}	$\geq 6.1 \times 10^{-12}$	4.1×10^{-11}	Cd	$<1.0 \times 10^{-14}$	$<3.3 \times 10^{-13}$	$<1.0 \times 10^{-14}$	Hg	2.4×10^{-13}	NA[a]	NA[a]

[a] NA = not available (Tc is radioactive, and $Hg^+ + C_6H_6 \rightarrow C_6H_6^+ + Hg$ with $k_{obs} = 6.7 \times 10^{-10}$ cm^3 molecule^{-1} s^{-1}).

generated using the ICP source, and they were allowed to add benzene upstream in the flow tube prior to reacting with molecular oxygen. Up to two molecules of benzene were observed to attach to most transition metal cations,[12] presumably by termolecular addition with helium buffer gas acting as a collisional stabilizing agent. Only Hg^+ did not form clusters with benzene and reacted instead by electron transfer because of its high recombination energy, $RE(Hg^+) = 10.44$ eV[14] compared with $IE(C_6H_6) = 9.24$ eV.[14] The recombination energies of most other transition metal cations are lower than 9.24 eV, thus preventing the electron-transfer channel. However, for Zn^+ [IE(Zn) = 9.39 eV],[14] the electron-transfer channel with benzene is also slightly exothermic, and it is observed to occur, but in competition with addition in a ratio of 4:10. The electron-transfer reaction with Au^+ is endothermic by only 0.01 eV [IE(Au) = 9.23 eV][14] and occurs in competition with adduct formation in a ratio of 2.5:10.

Measured ion profiles for benzene monoadducts of first-row transition metal ions reacting with oxygen are shown in Figure 1, and those for selected second-row and third-row transition metal ions are presented in Figure 2.

Table 1 summarizes the measured rate coefficients for the primary reactions with oxygen for both the mono- and bis-benzene adduct ions, $MC_6H_6^+$ and $M(C_6H_6)_2^+$, as well as for the bare metal cations M^+. The rate coefficients for reactions of benzene monoadducts with oxygen range from $<3.3 \times 10^{-13}$ to 4.4×10^{-10} cm^3 molecule^{-1} s^{-1} and are equal to, or lower than, the reaction rate coefficients for the bare early transition metal cations and higher than the reaction rate coefficients for the bare late transition metal cations. Rate coefficients for observed reactions of benzene bis-adducts range from 1.7×10^{-12} to 3.4×10^{-10} cm^3 molecule^{-1} s^{-1} and are lower than those for the bare and monoadduct ions except for Zn^+.

We have previously reported results for reactions of bare metal cations with O_2.[6] Two reaction channels were observed for the bare ions: O-atom transfer and O_2 addition, reactions 1a and 1b, respectively.

$$M^+ + O_2 \rightarrow MO^+ + O \quad (1a)$$

$$\rightarrow MO_2^+ \quad (1b)$$

Early transition metal cations were observed to react rapidly and exclusively by O-atom transfer, whereas late transition metal cations reacted slowly and only by molecular oxygen addition. O-atom transfer was found to be thermodynamically controlled, being fast when exothermic and slow when endothermic.

Several additional channels were observed to compete in reactions of benzene monoadducts with oxygen, reactions 2c−2g), and clear trends were observed across the periodic table.

$$MC_6H_6^+ + O_2 \rightarrow MC_6H_6O^+ + O \quad \text{O-atom transfer} \quad (2a)$$

$$\rightarrow MC_6H_6(O_2)^+ \quad \text{addition} \quad (2b)$$

$$\rightarrow MC_6H_4O^+ + H_2O \quad \text{addition/dehydration} \quad (2c)$$

$$\rightarrow C_6H_6^+ + MO_2 \quad \text{metal abstraction} \quad (2d)$$

$$\rightarrow MO_2^+ + C_6H_6 \quad \text{ligand switching} \quad (2e)$$

$$\rightarrow MC_4H_4^+ + (C_2H_2O_2) \quad \text{acetylene elimination} \quad (2f)$$

$$\rightarrow M^+ + (C_6H_6O_2) \quad \text{benzene abstraction} \quad (2g)$$

The benzene adducts of early transition metal cations reacted rapidly with oxygen ($k > 1.3 \times 10^{-10}$ cm^3 molecule^{-1} s^{-1}) and displayed up to five competing primary reaction channels. Reactions of most late transition metal cation−benzene adducts were slow ($k < 1.8 \times 10^{-10}$ cm^3 molecule^{-1} s^{-1}) and proceeded only by molecular oxygen addition. Only the benzene adducts of Ag^+ and Cd^+ were observed to be unreactive ($k < 1.6 \times 10^{-12}$ cm^3 molecule^{-1} s^{-1}), with no product ions detected in the flow range investigated. A separate category consists of reactions of benzene adducts of metal cations situated at the borderline between early and late transition metals. These reactions were relatively slow, but they resulted in many different primary product ions, most of which involved bimolecular activation of O−O, C−C, and C−H bonds.

Results obtained for primary reactions of transition metal cation−benzene adducts are presented in Figure 3 in the form of a periodic table and in Table 2. The periodic table displays branching ratios for the observed primary channels and reaction efficiencies expressed as the ratio of the measured rate coefficient (k_{obs}) and the collision rate coefficient (k_c) calculated with the algorithm of the modified variational transition state/classical trajectory theory developed by Su and Chesnavich.[15]

Secondary chemistry was observed only for transition metal cations from group 3B to group 8B and involved either O-atom transfer or molecular oxygen addition.

Reactions of metal cation−benzene bis-adducts with oxygen were also monitored. Only benzene bis-adducts of early transition metal cations and with Zn^+ were reactive, $k > 1.7 \times 10^{-12}$

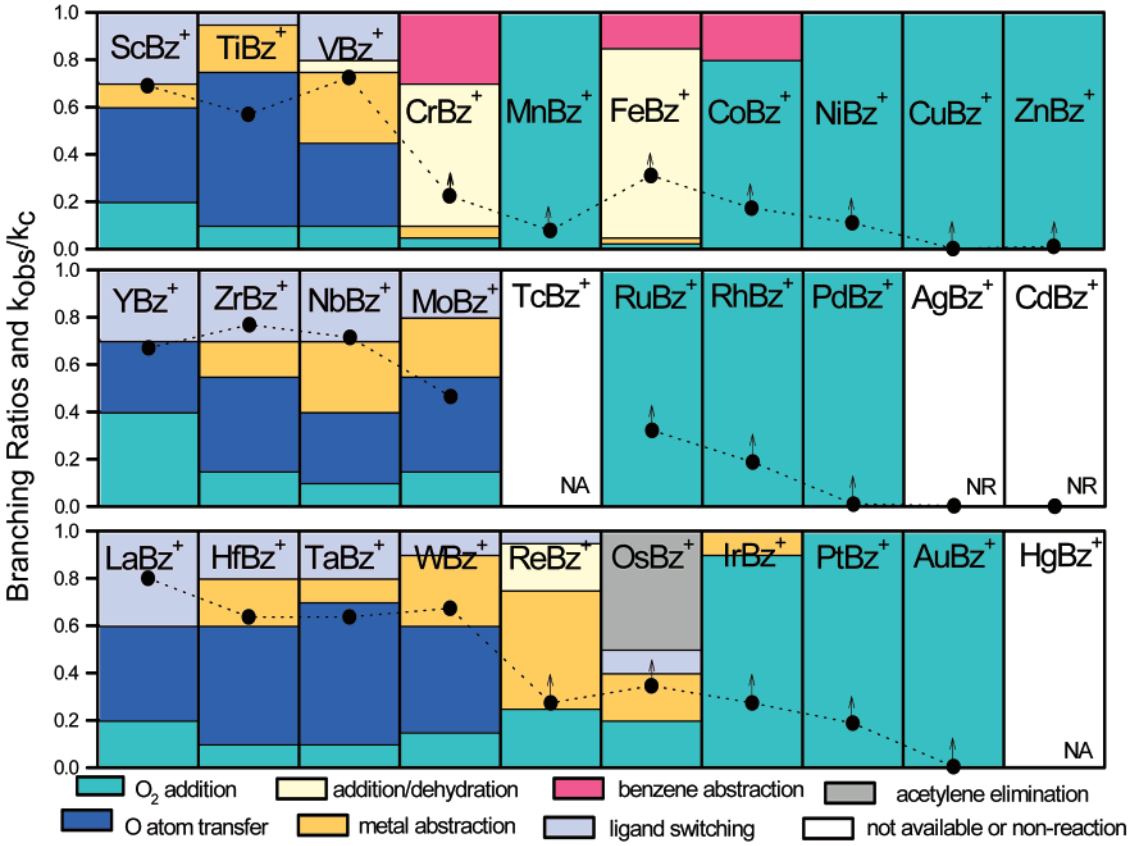

Figure 3. Periodic variations observed in the reactivities of transition metal ion−benzene monoadducts toward molecular oxygen, k_{obs}/k_c (represented as solid circles). k_{obs} represents the measured reaction rate coefficient (see Table 1), and k_c is the collision rate coefficient calculated with the algorithm of the modified variational transition state/classical trajectory theory developed by Su and Chesnavich.[15] Also indicated are the observed reaction channels (color coded) with their corresponding branching ratios given in a bar graph.

cm^3 $molecule^{-1}$ s^{-1}. Molecular oxygen addition, reaction 3a, O-atom transfer, reaction 3b, and ligand switching, reaction 3c, were observed.

$$M(C_6H_6)_2^+ + O_2 \rightarrow M(C_6H_6)_2O_2^+ \quad (3a)$$

$$\rightarrow M(C_6H_6)_2O^+ + O \quad (3b)$$

$$\rightarrow MC_6H_6(O_2)^+ + C_6H_6 \quad (3c)$$

Oxygen-Atom Transfer. O-atom transfer from molecular oxygen, reaction 2a, was observed in reactions of benzene adducts with transition metal cations from group 3B (Sc^+, Y^+, La^+), group 4B (Ti^+, Zr^+, Hf^+), group 5B (V^+, Nb^+, Ta^+), and group 6B (only Mo^+ and W^+). In all of these primary reactions, O-atom transfer was not the only channel observed, but it accounted for at least 30% of the reactive collisions (see Figure 3 and Table 2). The rate coefficients for the O-atom transfer channel, determined by multiplying the overall rate coefficients with the branching ratios for O-atom transfer, are all higher than 1.0×10^{-10} cm^3 $molecule^{-1}$ s^{-1}.

The reactions of the bare transition metal cations with oxygen resulting in O-atom transfer have been discussed previously.[6] Reaction 1a was observed to occur for Sc^+, Y^+, La^+, Ti^+, Zr^+, Hf^+, V^+, Nb^+, Ta^+, Mo^+, and W^+, transition metals that have oxygen-atom affinities higher or slightly lower than OA(O) = 119.1 ± 0.1 kcal mol^{-1}.[16] A strong correlation was found between reaction efficiency and exothermicity. The efficiency for O-atom transfer is high (>0.4) when exothermic and low (<0.1) when endothermic. The occurrence of O-atom transfer for benzene adducts of the same metal cations indicates that the process is a consequence of favorable thermochemistry of M^+−O bond formation and that the benzene ligand is not substantially involved in the activation of O_2.

Oxygen-atom transfer was also observed to occur as a secondary reaction, reaction 4, for M = Nb, Mo, Ta, and W.

$$MC_6H_6O^+ + O_2 \rightarrow MC_6H_6O(O)^+ + O \quad (4)$$

$NbC_6H_6O^+$, $MoC_6H_6O^+$, $TaC_6H_6O^+$, and $WC_6H_6O^+$ all reacted with O_2 by O-atom transfer with reaction efficiencies equal to unity. Previous studies[6] in our laboratory showed that the bare metal oxide cations that react with O_2 by O-atom transfer are NbO^+, MoO^+, TaO^+, and WO^+. Reaction efficiencies were determined to range from 0.63 to 0.97, in line with high reaction exothermicities calculated from the available data.[16] Again, these results taken together suggest that the benzene ligand makes little contribution in the activation of oxygen and has essentially no effect on the oxygen-atom affinity of the metal cation. According to the thermochemical cycle shown in Scheme 1, the O-atom affinity of $MC_6H_6^+$, $OA(MC_6H_6^+)$, is related to $OA(M^+)$ according to eq 5, where BA represents the benzene affinity.

$$OA(MC_6H_6^+) = OA(M^+) + BA(MO^+) - BA(M^+) \quad (5)$$

Because the difference in benzene affinity $BA(MO^+) - BA(M^+)$ is not expected to be large, the difference in O-atom affinity $OA(MC_6H_6^+) - OA(M^+)$ is also likely not to be large.

O_2 Addition. All reactive benzene monoadducts displayed the molecular oxygen addition channel, reaction 2b (see Tables 2 and 3 and Figure 3). O_2 addition was observed to compete with other reaction channels in the reactions with benzene mono-

TABLE 2: Reaction Efficiencies for Primary Reactions with O_2 of Benzene Mono-Adducts of Transition Metal Cations, k_{obs}/k_c, and Branching Ratios for Observed Primary Product Ions (BR in %) in He at 0.35 ± 0.01 Torr and 295 ± 2 K

	k_{obs}/k_c[a]	BR[b]($MC_6H_6O_2^+$)	BR($MC_6H_6O^+$)	BR($MC_6H_4O^+$)	BR($C_6H_6^+$)	BR(MO_2^+)	BR(M^+)	BR($MC_4H_4^+$)
$ScC_6H_6^+$	0.69	20	40		10	30		
$YC_6H_6^+$	0.67	40	30			30		
$LaC_6H_6^+$	0.80	20	40			40		
$TiC_6H_6^+$	0.57	10	65		20	5		
$ZrC_6H_6^+$	0.77	15	40		15	30		
$HfC_6H_6^+$	0.64	10	50		20	20		
$VC_6H_6^+$	0.72	10	35	5	30	20		
$NbC_6H_6^+$	0.71	10	30		30	30		
$TaC_6H_6^+$	0.64	10	60		10	20		
$CrC_6H_6^+$	≥0.22	5		60	5		30	
$MoC_6H_6^+$	0.46	15	40		25	20		
$WC_6H_6^+$	0.67	15	45		30	10		
$MnC_6H_6^+$	≥0.08	100						
$ReC_6H_6^+$	≥0.27	25		20	50	5		
$FeC_6H_6^+$	≥0.31	2.5		80	2.5		15	
$RuC_6H_6^+$	≥0.32	100						
$OsC_6H_6^+$	≥0.35	20			20	10		50
$CoC_6H_6^+$	≥0.17	80					20	
$RhC_6H_6^+$	≥0.19	100						
$IrC_6H_6^+$	≥0.27	90			10			
$NiC_6H_6^+$	≥0.11	100						
$PdC_6H_6^+$	$\geq 9.6 \times 10^{-3}$	100						
$PtC_6H_6^+$	≥0.19	100						
$CuC_6H_6^+$	$\geq 1.1 \times 10^{-3}$	100						
$AgC_6H_6^+$	$<2.8 \times 10^{-3}$	-						
$AuC_6H_6^+$	$\geq 3.8 \times 10^{-3}$	100						
$ZnC_6H_6^+$	≥0.01	100						
$CdC_6H_6^+$	$<5.9 \times 10^{-4}$	-						

[a] k_c = collision rate coefficient calculated with the algorithm of the modified variational transition state/classical trajectory theory developed by Su and Chesnavich.[15] [b] BR = zero-flow intercepts of primary product ions from plots of relative abundance of product ions as a function of O_2 flow.

SCHEME 1

$$MO^+ + C_6H_6 \rightarrow M^+ + O + C_6H_6$$
$$\downarrow \qquad\qquad \uparrow$$
$$C_6H_6MO^+ \rightarrow C_6H_6M^+ + O$$

adducts of the *early* transition metal cations from groups 3−6 within the range from only 5% (for $CrC_6H_6^+$) to 40% (for $YC_6H_6^+$). Competition was also observed in the reactions of $MC_6H_6^+$ for M = Fe, Co, Re, Os, and Ir. Exclusive O_2 addition was seen with Mn^+ and all other *late* transition metal ions (see Figure 3). No O_2 addition was seen for the adducts with M = Ag and Cd.

The effective bimolecular reaction rate coefficients for the O_2 addition channel with benzene monoadducts range from $\geq 6.6 \times 10^{-13}$ cm^3 molecule^{-1} s^{-1} (for $CuC_6H_6^+$) to $\geq 1.8 \times 10^{-10}$ cm^3 molecule^{-1} s^{-1} (for $RuC_6H_6^+$). When compared with the results obtained for bare late transition metal cations, the rates for O_2 addition are enhanced by up to 4 orders of magnitude (see Table 3) with the attachment of benzene to the metal cation. The addition channel (reaction 2b) is presumed to occur under SIFT conditions at 0.35 Torr of He by collisional stabilization rather than by radiative association. The presence of the benzene ligand increases the number of degrees of freedom in the intermediate formed with O_2 and thus enhances the rate coefficient for the addition reaction.[17]

One molecule of oxygen was observed to attach to most benzene monoadducts. Only the Sc^+ and Y^+ benzene monoadducts added two molecules of O_2 sequentially to form $MC_6H_6O_2(O_2)^+$, consistent with their capability to accept the largest number of electrons (in rows 1 and 2) to fill their valence shells.

O_2 addition was also observed to occur with monoxide cations formed in reaction 2a. $TiC_6H_6O^+$, $ZrC_6H_6O^+$, $HfC_6H_6O^+$, and $VC_6H_6O^+$ all reacted relatively rapidly (see Table 3) by adding one molecule of O_2 according to reaction 6, $k > 7.9 \times 10^{-11}$ cm^3 molecule^{-1} s^{-1}.

$$MC_6H_6O^+ + O_2 \rightarrow MC_6H_6O(O_2)^+ \qquad (6)$$

In contrast, the group-three $MC_6H_6O^+$ (M = Sc, Y, and La) cations were observed not to add O_2, nor to abstract an O atom. This behavior can be attributed to the special stability expected for these cations on the basis of the expected stability of the bare metal oxide cations as discussed for ScO^+ by Schröder et al.[2a,] and Fisher et al.[18] ScO^+ has all bonding molecular orbitals doubly occupied and all nonbonding and antibonding orbitals empty.

Equilibrium analyses performed on the kinetic results indicate that equilibrium is attained in the O_2 addition reactions to monobenzene adducts of most late transition metal cations. These analyses are based on plots of product-to-reactant ion signal ratios as a function of reactant flow. Equilibrium is achieved when the plot achieves linearity because [product$^+$]/[reactant$^+$] = K_{eq}[O_2]. Calculated equilibrium constants, K_{eq} (standard state = 1 atm), are presented in Table 3, along with the corresponding change in standard free energy, $\Delta G°$. Also, limiting values for K_{eq} and $\Delta G°$ are included for reactions that did not achieve equilibrium, in many cases because of competing reaction

TABLE 3: Reaction Rate Coefficients for O_2 Addition (k_{add} in cm^3 molecule^{-1} s^{-1}), Equilibrium Constants for Addition Reactions at a Standard State of 1 atm (K_{eq}) and Standard Free Energies for the Ligation Reactions ($\Delta G°$ in kcal mol^{-1}) in He at 0.35 ± 0.01 Torr and 295 ± 2 K

	M^+	$MC_6H_6^+$			$MC_6H_6O^+$			$M(C_6H_6)_2^+$		
M	k_{add}	k_{add}	K_{eq}	$\Delta G°$	k_{add}	K_{eq}	$\Delta G°$	k_{add}	K_{eq}	$\Delta G°$
Sc	–[a]	8.0×10^{-11}	$>1.2 \times 10^7$	<-9.6	–			4.4×10^{-11}	$>4.4 \times 10^6$	<-9.1
Ti	–	3.3×10^{-11}	$>6.6 \times 10^7$	<-10.7	3.3×10^{-10}	$>1.3 \times 10^8$	<-11.0	–		
V	–	4.2×10^{-11}	$>1.6 \times 10^8$	<-11.2	7.9×10^{-11}	$>2.1 \times 10^7$	<-9.8	–		
Cr	2.2×10^{-13}	$\geq 6.5 \times 10^{-12}$	$>2.9 \times 10^6$	<-8.8	–			–		
Mn	$<1.0 \times 10^{-14}$	$\geq 4.5 \times 10^{-11}$	1.3×10^7	-9.7	–			–		
Fe	4.3×10^{-13}	$\geq 4.5 \times 10^{-12}$	$>3.7 \times 10^7$	<-10.3	–			–		
Co	1.5×10^{-13}	$\geq 8.0 \times 10^{-11}$	5.5×10^7	-10.5	–			–		
Ni	5.0×10^{-14}	$\geq 6.4 \times 10^{-11}$	2.9×10^7	-10.2	–			–		
Cu	2.6×10^{-13}	$\geq 6.6 \times 10^{-13}$	6.3×10^4	-6.5	–			–		
Zn	2.7×10^{-13}	$\geq 6.1 \times 10^{-12}$	4.4×10^5	-7.8	–			4.1×10^{-11}	$>1.3 \times 10^7$	<-9.7
Y	–	1.5×10^{-10}	$>2.5 \times 10^7$	<-10.1	–			1.8×10^{-10}	2.7×10^7	-10.1
Zr	–	6.5×10^{-11}	$>5.2 \times 10^7$	<-10.5	1.3×10^{-10}	$>6.9 \times 10^7$	<-10.7	6.2×10^{-11}	$>4.3 \times 10^6$	<-9.1
Nb	–	4.0×10^{-11}	–	–	–			5.4×10^{-12}	4.7×10^5	-7.7
Mo	–	3.9×10^{-11}	–	–	–			–		
Ru	1.6×10^{-13}	$\geq 1.8 \times 10^{-10}$	6.4×10^7	-10.6	–			–		
Rh	1.9×10^{-14}	$\geq 1.1 \times 10^{-10}$	3.3×10^7	-10.3	–			–		
Pd	1.5×10^{-14}	$\geq 5.4 \times 10^{-12}$	5.9×10^5	-7.9	–			–		
Ag	4.5×10^{-13}	$< 1.6 \times 10^{-12}$	–	–	–			–		
Cd	$<1.0 \times 10^{-14}$	$<3.3 \times 10^{-13}$	–	–	–			–		
La	–	8.8×10^{-11}	$>1.2 \times 10^8$	<-11.0	–			3.4×10^{-10}	$>3.6 \times 10^7$	<-10.3
Hf	–	3.5×10^{-11}	$>2.1 \times 10^7$	<-10.0	1.8×10^{-10}	$>5.3 \times 10^7$	<-10.5	1.6×10^{-11}	$>8.1 \times 10^5$	<-8.1
Ta	–	1.1×10^{-10}	–	–	–			1.7×10^{-12}	$>5.4 \times 10^6$	<-9.2
W	–	5.6×10^{-11}	–	–	–			–		
Re	1.1×10^{-12}	$\geq 3.8 \times 10^{-11}$	$>1.4 \times 10^7$	<-9.7	–			–		
Os	1.6×10^{-12}	$\geq 3.8 \times 10^{-11}$	$>7.8 \times 10^6$	<-9.4	–			–		
Ir	7.1×10^{-14}	$\geq 4.5 \times 10^{-11}$	3.3×10^7	-10.3	–			–		
Pt	1.0×10^{-14}	$\geq 1.1 \times 10^{-10}$	4.4×10^7	-10.4	–			–		
Au	1.4×10^{-13}	$\geq 2.1 \times 10^{-12}$	–	–	–			–		

[a] No reaction, $k < 1 \times 10^{-14}$ cm^3 molecule^{-1} s^{-1}.

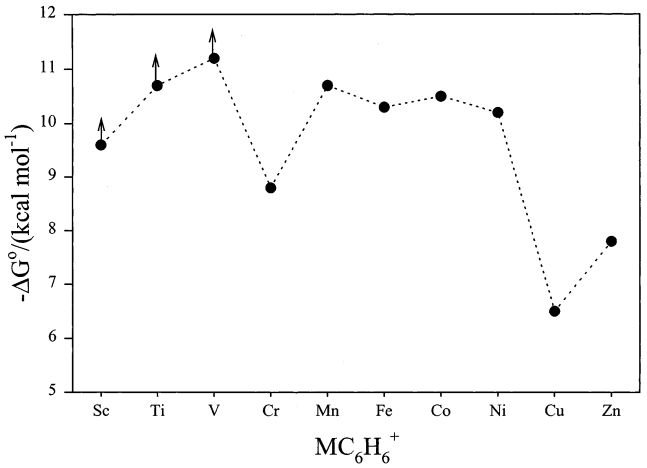

Figure 4. Variation in the standard free energy change, $\Delta G°$, determined from equilibrium constant measurements for O_2 addition to benzene adducts, $MC_6H_6^+$, of the first-row transition metal cations.

channels. Rate coefficients for reactions that achieve equilibrium are reported as lower limits in Tables 1−3. The variation in $\Delta G°$ for O_2 addition to benzene adducts of the first-row transition metal cations is presented in Figure 4. The "doubly humped" shape of this plot is very familiar and can be associated with trends in binding energies of transition metal cations with various other ligands.[19−21] The lowest values for $-\Delta G°$ are observed for metal cations that exhibit d^5 (Cr^+ and Mn^+) or d^{10} (Cu^+ and Zn^+) configurations.

Addition/Dehydration. A third type of primary reaction channel observed in reactions of $MC_6H_6^+$ and oxygen is the addition of molecular oxygen followed by water elimination (reaction 2c). Only the benzene monoadducts of V^+, Cr^+, Fe^+ and Re^+ show such a reaction pathway, which accounted for 5, 60, 80, and 20%, respectively, of the reactive collisions. Measured rate coefficients that correspond to this channel alone were 2.1×10^{-11}, $\geq 7.8 \times 10^{-11}$, $\geq 1.4 \times 10^{-10}$, and $\geq 3.0 \times 10^{-11}$ cm^3 molecule^{-1} s^{-1}, respectively. Kinetic results for the reactions of $CrC_6H_6^+$ and $FeC_6H_6^+$ are presented in Figure 5. The curvature in the semilogarithmic decays of $CrC_6H_6^+$ and $FeC_6H_6^+$ is attributed to the occurrence of the reverse of the oxygen-addition reaction and the addition of benzene in the reaction region to the free metal ion produced in reaction 2g.

The bond connectivities in the resulting $MC_6H_4O^+$ ions were investigated using our multicollision CID method for M = Cr and Fe for which the addition/dehydration reaction pathway was a major primary channel. Figure 6 indicates that the multicollision-induced dissociation of $CrC_6H_4O^+$ in Ar buffer gas results in the formation of Cr^+ accompanied by the loss of (C_6H_4O), whereas dissociation of $FeC_6H_4O^+$ under similar conditions results in loss of CO and formation of $FeC_5H_4^+$. The observed subsequent dissociation of $FeC_5H_4^+$ involves loss of acetylene with formation of $FeC_3H_2^+$. A similar dissociation pattern that also involves loss of CO and C_2H_2 was reported by Schwarz and co-workers for the dissociation of $FeC_6H_4O^+$ produced in the reaction of Fe^+ with dihydroxybenzene[22] and for the dissociation of $FeC_6H_4O^+$ formed in the reaction of FeO^+ with phenol.[23] These authors performed isotope-labeling experiments, extensive MS/MS studies, and collision-induced dissociation studies with related $FeC_6H_4O^+$ ions (with the same molecular formula but different structures) generated by independent routes. On this basis, they suggested that structure **1** is the most probable structure for $FeC_6H_4O^+$ that loses CO and C_2H_2 in

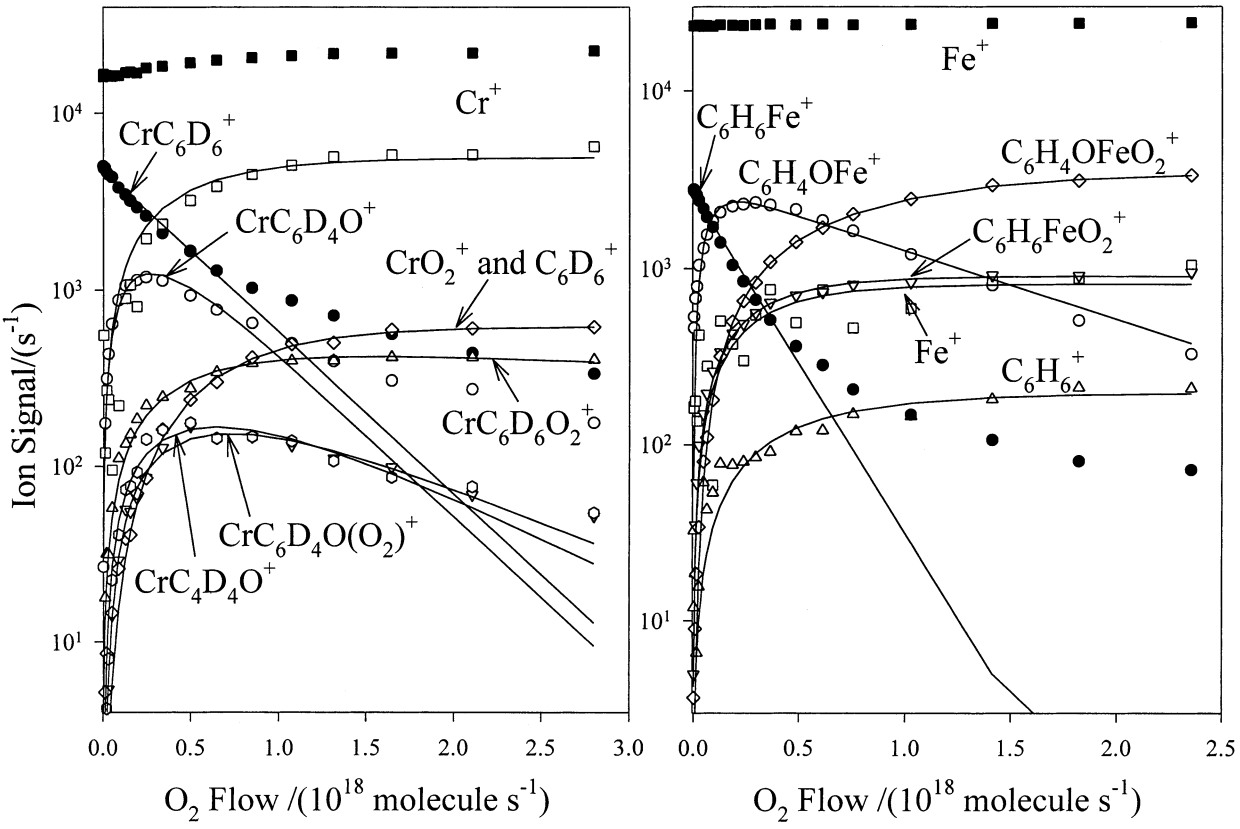

Figure 5. Reactant and product ion intensities observed for the reactions of $CrC_6D_6^+$ and $FeC_6H_6^+$ with O_2. The data were fit using sequential first-order kinetics for the mechanism described in the text. The ion intensities for Cr^+ and Fe^+ are represented by filled squares; the open squares represent the signal intensities for the same metal cations after subtraction of the initial signal.

CID experiments. Therefore, we suggest that $FeC_6H_4O^+$ formed in channel 2c has this structure as well.

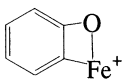

(1)

The observed dissociation of $CrC_6H_4O^+$ into $Cr^+ + (C_6H_4O)$ (see Figure 6) indicates a different bond connectivity within this molecular ion, probably with the metal cation coordinated to an oxirene ring (**2**) or to a keto-carbene (**3**), which can result from **2** through a Wolff rearrangement.[24]

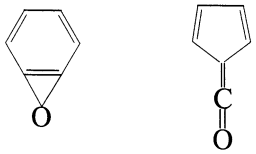

(2) **(3)**

Both of the suggested structures for the $MC_6H_4O^+$ ions (M = Cr, Fe) produced in reaction 2c involve oxidation of the benzene ring. The same is likely for M = V and Re, for which CID experiments were not possible because of low product intensities. Thus, channel 2c is distinct from channels 2a and 2b, which result in the formation of the monoxide and dioxide of the metal cations coordinated to benzene.

The $CrC_6H_4O^+$ and $FeC_6H_4O^+$ ions produced in reaction 2c were observed to add O_2: two molecules of O_2 attached sequentially to $CrC_6H_4O^+$, whereas only one molecule added to $FeC_6H_4O^+$. This difference in the number of oxygen molecules added can be attributed to a difference in the electronic configurations of the metal ions (Cr^+ can accept one more electron), or it might simply be a manifestation of the two different structures assigned to $CrC_6H_4O^+$ and $FeC_6H_4O^+$.

Metal Abstraction. Reaction 2d was observed in 14 of the 28 reactions investigated. Figure 3 shows that reaction 2d occurs mainly with the benzene adducts of early transition metal cations, but it also occurs with some late transition metal−benzene cations. The branching ratio for this channel varied from 2.5% (for $FeC_6H_6^+$) to 50% (for $ReC_6H_6^+$).

Reaction 2d is exothermic if $D(M-O_2) > IE(C_6H_6) - IE(M) + D(M^+-C_6H_6)$. The observation of reaction 2d for 14 metals implies *exothermicity* for these reactions and so can be used to provide lower limits to $D(M-O_2)$, at least for the five metals for which values for $D(M^+-C_6H_6)$ are available. These values are given in Table 4, along with known values for IE(M) and $D(M^+-C_6H_6)$. Transition metal cation−benzene bond energies have been determined both experimentally and computationally.[19,27,28] The ionization energy of benzene is taken to be 9.24 eV.[14] The assumption of *endothermicity* for those 14 reactions of type 2d that were observed *not to occur* provides the upper limits for $D(M-O_2)$ given in Table 4 for the eight metals for which values of $D(M^+-C_6H_6)$ are available. These upper limits are not meaningful if causes other than endothermicity lead to nonreaction. Because $D(M-O_2) = \Delta H_f^o(M) - \Delta H_f^o(MO_2)$, limits for $\Delta H_f^o(MO_2)$ have also been calculated and are shown in Table 4.

The metal-abstraction reaction produces neutral metal dioxide, and this bond formation can be conceived to promote endo-

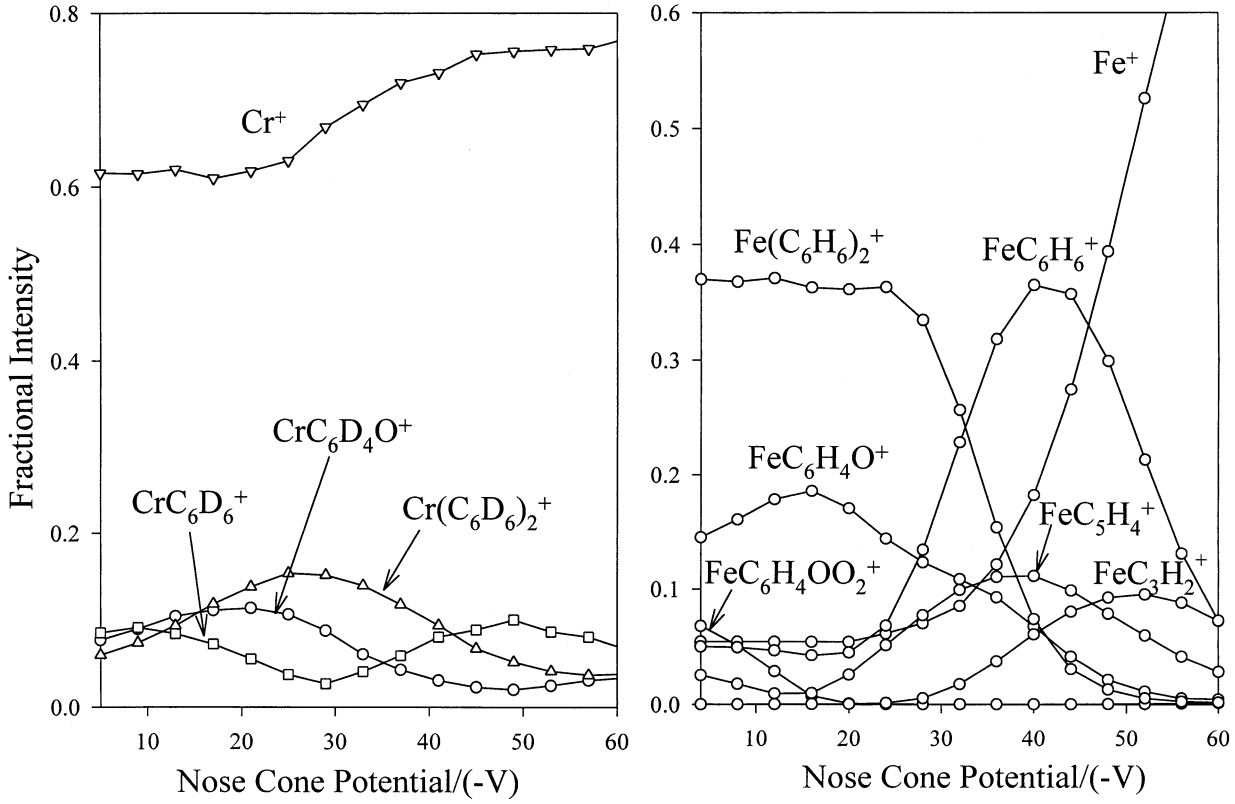

Figure 6. Multicollision-induced dissociation spectra for $CrC_6D_4O^+$ and $FeC_6H_4O^+$ in Ar buffer gas at 0.092 Torr.

thermic electron transfer between the metal ion and benzene as illustrated in reaction sequence 7a−7c.

$$M^+ + C_6H_6 \rightarrow MC_6H_6^+ \quad (7a)$$

$$MC_6H_6^+ + O_2 \rightarrow C_6H_6^+ + MO_2 \quad (7b)$$

$$M^+ + C_6H_6 + O_2 \rightarrow C_6H_6^+ + MO_2 \quad (7c)$$

Reaction 7c can now be used to determine lower limits for $D(M-O_2)$ for those metals for which $D(M^+-C_6H_6)$ is not known because $D(M-O_2) > IE(C_6H_6) - IE(M)$ if reaction 7c is exothermic. Reaction 7c is exothermic when both reactions 7a and 7b are exothermic, which can be assumed to be the case when reaction 7b (or 2d) is observed. The results are included in Table 4.

Ligand Switching. The ligand-switching reactions 2e were observed for 13 of the 28 systems investigated, mostly involving early transition metal cations. We have labeled this formally as a "ligand-switching" reaction although other mechanisms are possible. For example, metal-atom abstraction followed by intramolecular electron transfer prior to separation according to reaction 8 is another possibility.

$$C_6H_6M^+ + O_2 \rightarrow [C_6H_6M^+\cdots O_2 \rightarrow C_6H_6\cdots M^+O_2] \rightarrow MO_2^+ + C_6H_6 \quad (8)$$

In any case, the branching ratios for this channel varied from 5% for Ti and Re to 40% for La.

The occurrence of the ligand-switching reaction 2e implies that $D(M^+-C_6H_6) < D(M^+-O_2)$. The lower limits for $D(M^+-O_2)$ given in Table 4 were estimated from the observation of reaction 2e—which implies *exothermicity*—for those metal cations with known binding energies to benzene. The non-observation of reaction 2e was taken as an indication of *endothermicity*, and upper limits for bond energies $D(M^+-O_2)$ were estimated, giving the results shown in Table 4. Limits for $\Delta H_f(M^+O_2)$ were calculated from $D(M^+-O_2) = \Delta H_f^o(M^+) - \Delta H_f^o(M^+O_2)$ (see Table 4).

The sequence of benzene adduct formation followed by ligand switching described in the reaction scheme 9a−9c provides an alternative route for the association of O_2 to atomic metal ions.

$$M^+ + C_6H_6 \rightarrow MC_6H_6^+ \quad (9a)$$

$$MC_6H_6^+ + O_2 \rightarrow MO_2^+ + C_6H_6 \quad (9b)$$

$$M^+ + O_2 \rightarrow MO_2^+ \quad (9c)$$

As the rate for direct association is limited by the small number of degrees of freedom of the intermediate $(MO_2^+)^*$ involved in this association, benzene is likely to serve as a catalyst. Benzene addition to metal ions is considerably more efficient because of the higher number of degrees of freedom.

Benzene Abstraction. Reaction 2g was observed to occur for $CrC_6H_6^+$, $FeC_6H_6^+$, and $CoC_6H_6^+$ with molecular oxygen and to result in regeneration of the bare metal cation. Branching percentages of 30, 15, and 20%, respectively, were measured for this channel for Cr, Fe, and Co, respectively. The neutral product presumably results from the oxidation of benzene because the observation of this channel implies that it is exothermic. The production of $M^+ + C_6H_6 + O_2$ would be endothermic.

The overall chemistry can be described by the reaction sequence 10a−10c. Reactions 10a and 10b constitute a catalytic

TABLE 4: Literature Ionization Energies, Enthalpies of Formation at 298 K, and Bond Dissociation Energies and Estimated Limits for Bond Dissociation Energies and Enthalpies of Formation (in kcal mol^{-1}) Derived from the Endothermicities/ Exothermicities of Reactions 2d and 2e

M	IE(M)[a]	$D(M-O_2)$[b]	$\Delta H_f^o(M)$[c]	$\Delta H_f^o(MO_2)$[b]	$D(M^+-C_6H_6)$[d]	$D(M^+-O_2)$[b]	$\Delta H_f^o(M^+)$[f]	$\Delta H_f^o(M^+O_2)$[b]
Ti	157.5	>118.5	113	<−5.5	62.8	>62.8	270.5	<207.7
V	155.6	>108.7	123.2	<14.5	51.1	>51.1	278.8	<227.7
Cr	156.0	>94.5	95.0	<0.5	37.4	>37.4	251.0	<213.6
Zr	153.0	>60.2	145.8	<85.6			298.8	
Nb	155.9	>109.4	175.2	<65.8	52.1	>52.1	331.1	<279.0
Mo	163.6	>49.6	157.5	<107.9			321.1	
Ta	174.1	>39.1	186.9	<147.8			361.0	
W	181.3	>31.8	203.4	<171.6			384.7	
Sc	151.3	>61.9	90	<28.1			241.3	
Hf	157.4	>55.8	147.8	<92.0			305.2	
Re	180.6	>32.5	184	<151.5			364.6	
Os	194.9	>18.6	189	<170.4			383.9	
Fe	182.2	>82.0	99.3	<17.3	51.1	<51.1	281.5	>230.4
Ir	206.8	>6.4	159	<152.6			365.8	
Y	143.4	<110.6	101	>−9.6	40.8	>40.8	244.4	<203.6
La	128.6		103				231.6	
Rh	172.0		133				305.0	
Pt	206.6		135				341.6	
Mn	171.4	<76.8	67	>−9.8	35.1	<35.1	238.4	>203.3
Co	181.7	<94.0	102	>8.0	62.6	<62.6	283.7	>221.1
Ni	176.2	<96.3	102.8	>6.5	59.3	<59.3	279.0	>219.7
Cu	178.8	<86.1	80.9	>−5.2	51.1	<51.1	259.7	>208.6
Zn	216.6		31.2				247.8	
Ru	169.7	<92.1	154	>61.9	48.7	<48.7	323.7	>275.0
Pd	192.2		90				282.2	
Ag	174.7	<75.0	68.0	>−7.0	36.5	<36.5	242.7	>206.2
Cd	207.4		26.8				234.2	
Au	212.7	<61.5	87	>25.5	61.1[e]	<61.1	299.7	>238.6

[a] Literature values taken from ref 26. [b] Estimated in this work. [c] Literature values taken from ref 14. [d] Taken from ref 27 unless otherwise specified. [e] Taken from ref 28. [f] $\Delta H_f^o(M^+) = \Delta H_f^o(M) + IE(M)$.

cycle in which benzene is oxidized.

$$M^+ + C_6H_6 \rightarrow MC_6H_6^+ \quad (10a)$$

$$MC_6H_6^+ + O_2 \rightarrow M^+ + (C_6H_6O_2) \quad (10b)$$

$$C_6H_6 + O_2 \rightarrow (C_6H_6O_2) \quad (10c)$$

The oxidation of benzene with molecular oxygen has at least several exothermic channels, as shown in Scheme 2. Thermochemical information for the species involved in Scheme 2 was obtained from refs 16 and 29. However, benzene is not readily oxidized at room temperature.[29] The reaction is spin-forbidden because ground-state O_2 is a triplet and benzene is a singlet.[29] Several examples are known in biology and industry in which this reaction is catalyzed.[4] For example, carcinogenic and neurotoxic organopolluants such as benzene, toluene, xylenes, ethylbenzene, and chlorinated derivatives are mineralized in water and soil by bacterial strains from the *Pseudomonas* family.[29,30a,b] The most exothermic channel in Scheme 2 involves the generation of 1,2-dihydroxybenzene (catechol). Catechol is a major oxidation metabolite of benzene that is usually generated from the catalytic action of an iron-containing dioxygenase metalloenzyme.[30a,b] Also, depending on the catalyst used in the industrial oxidation of benzene, catechol can be the major reaction product (along with quinones), to the detriment of the production of phenol.[31]

Schwarz and co-workers have studied the gas-phase oxidation of benzene mediated by first-row transition metal oxide cations,[32a,b] and they also have identified reaction channels that regenerate the metal cation and, presumably, produce neutral phenol. They have shown that CrO^+, CoO^+, and FeO^+ react with benzene mainly by O-atom transfer to benzene to produce neutral phenol and the metal cation. The metal oxide cations

SCHEME 2

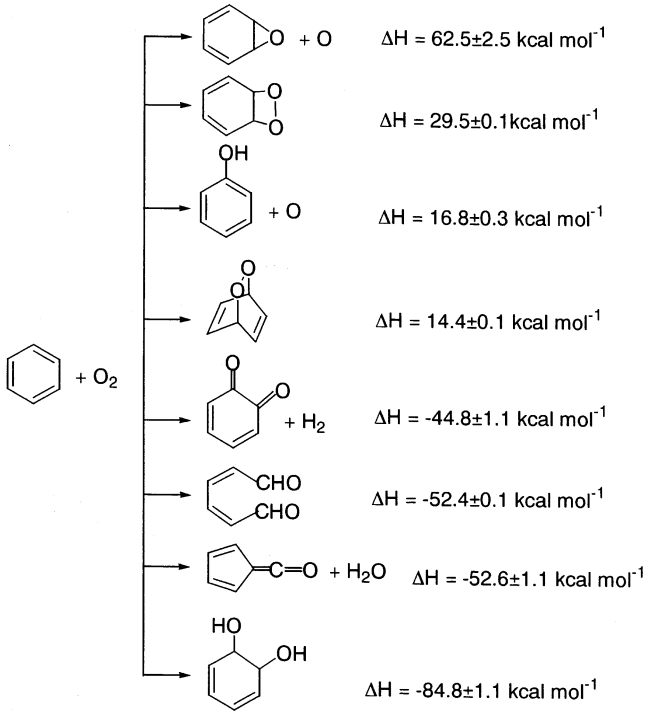

were produced from the reaction of the metal cation with N_2O, but Cr^+ and Co^+ had to be translationally excited for this to take place. In the ground state, only Fe^+ initiated a catalytic cycle involving FeO^+ as an intermediate. In contrast, when the unexcited metal ion was first attached to benzene and then reacted with N_2O, Cr^+ and Co^+ were regenerated, but not Fe^+.[32b]

The Schwarz group has also studied the oxidation with O_2 of $FeC_6H_6^+$ produced from the ligand-exchange reaction

between $FeC_2H_4^+$ and benzene.[33] Although $FeC_2H_4^+$ was observed to regenerate Fe^+ in reaction with oxygen, $FeC_6H_6^+$ did not. Instead, $FeC_6H_6^+$ reacted with O_2 to produce $C_5H_6OFe^+$ (+ CO) and $C_5H_4Fe^+$ (+ CO + H_2O). We did not observe these channels (see Figure 3 and Table 2), which require considerable bond redisposition.

Reactions of $M(C_6H_6)_2^+$. The benzene bis-adducts of all transition metal cations (except Tc^+ and Hg^+) were generated by adding sufficient benzene vapor upstream in the flow tube to deplete both M^+ and $MC_6H_6^+$ and, so, to eliminate effects due to reactions of these precursor ions. Only benzene bis-adducts of early transition metal cations (Sc^+, Y^+, La^+, Zr^+, Hf^+, Nb^+, and Ta^+) and the late transition metal cation Zn^+ were observed to react with molecular oxygen. Reaction rate coefficients (see Table 1) range from 1.7×10^{-12} cm^3 $molecule^{-1}$ s^{-1} for $Ta(C_6H_6)_2^+$ to 3.4×10^{-10} cm^3 $molecule^{-1}$ s^{-1} for $La(C_6H_6)_2^+$.

For $Zn(C_6H_6)_2^+$, $Nb(C_6H_6)_2^+$, and $Ta(C_6H_6)_2^+$, addition of one molecule of O_2 was the only reaction observed. $Sc(C_6H_6)_2^+$ and $Y(C_6H_6)_2^+$ sequentially added two molecules of O_2. The formation of the $M(C_6H_6)_2(O_2)_2^+$ adduct was observed to compete with ligand switching according to reactions 11a and 11b in a ratio of 1:1.

$$M(C_6H_6)_2(O_2)^+ + O_2 \rightarrow M(C_6H_6)_2(O_2)_2^+ \quad (11a)$$

$$\rightarrow MC_6H_6O_2(O_2)^+ + C_6H_6 \quad (11b)$$

$La(C_6H_6)_2^+$ reacted by adding one molecule of O_2 in competition with O-atom transfer in a ratio of 1:1 according to reactions 12a and 12b.

$$La(C_6H_6)_2^+ + O_2 \rightarrow La(C_6H_6)_2(O_2)^+ \quad (12a)$$

$$\rightarrow La(C_6H_6)_2O^+ + O \quad (12b)$$

$Zr(C_6H_6)_2^+$ and $Hf(C_6H_6)_2^+$ showed three reaction channels: addition (of one molecule of O_2), O-atom transfer (followed by addition of O_2), and ligand-switching according to reactions 13a−13c.

$$M(C_6H_6)_2^+ + O_2 \rightarrow M(C_6H_6)_2(O_2)^+ \quad (13a)$$

$$\rightarrow M(C_6H_6)_2O^+ + O \quad (13b)$$

$$\rightarrow MC_6H_6(O_2)^+ + C_6H_6 \quad (13c)$$

These three competing primary reaction channels occurred with approximately equal branching ratios.

Figure 7 presents a composite of reaction profiles for benzene bis-adducts of Sc^+, Nb^+, La^+ and Zn^+ reacting with O_2. The decays of the corresponding benzene monoadducts monitored in separate (low-flow) experiments are also indicated for comparison of reactivities of the mono- and bis-benzene adducts. Most reactions of $M(C_6H_6)_2^+$ with O_2 are slower than the corresponding reactions of $MC_6H_6^+$ with O_2 (see Table 1). However, the benzene bis-adducts $La(C_6H_6)_2^+$ and $Y(C_6H_6)_2^+$ reacted with rate coefficients comparable to those for the reactions of the corresponding benzene monoadducts. One bis-adduct, $Zn(C_6H_6)_2^+$, reacted *more rapidly* than its benzene monoadduct.

The differences in the rates of reaction of bis-adducts with O_2 are difficult to rationalize without knowledge of their structures and, thus, the accesssibilities of the metal cations. A sandwich structure would decrease this accessibility relative to a half-sandwich structure and, so, would reduce the rate of O_2 addition. The inverse behavior observed with Zn^+ is somewhat puzzling, but we note that only for this transition metal is IE(Zn) > IE(benzene). Partial electron transfer to the benzene ligands could therefore occur and the O_2 addition might then take place on one of the partially charged benzene ligands.

The different numbers of molecules of O_2 added to the $M(C_6H_6)_2^+$ clusters can be understood in terms of the different electronic configurations of the metal cations. $Sc(C_6H_6)_2O_2O_2^+$ and $Y(C_6H_6)_2O_2O_2^+$ obtained from the sequential addition of two O_2 molecules to the benzene bis-adducts of Sc^+ and Y^+ are stable 18-electron species, but so are $Nb(C_6H_6)_2O_2^+$ and $Ta(C_6H_6)_2O_2^+$ obtained from single addition of O_2 to $Nb(C_6H_6)_2^+$ and $Ta(C_6H_6)_2^+$. The addition of another molecule of O_2 to any of the four oxygenated complexes would generate unstable 20-electron species, and such additions were not observed.

The observation of an O-atom transfer channel in the reactions of the benzene bis-adducts of La^+, Zr^+, and Hf^+ with O_2 is interesting, although not surprising, because bare La^+, Zr^+, and Hf^+ have the highest O-atom affinities (206 ± 4, 178.9 ± 2.5 and 173 ± 5 kcal mol^{-1}, respectively)[2a] among the transition metal cations investigated. The results obtained for the O-atom transfer reactions observed with $MC_6H_6^+$ indicate that the presence of one molecule of benzene coordinated to these metal cations does not lower their O-atom affinity below $OA(O) = 119.1 \pm 0.1$ kcal mol^{-1}.[16] However, the coordination of two molecules of benzene to a metal cation leads to the disappearance of the O-atom transfer reaction channel for metal cations with $OA(M^+) < 173 \pm 5$ kcal mol^{-1}. $Ta(C_6H_6)_2^+$ did not react by O-atom transfer, even though the OA of Ta^+ is 188 ± 15 kcal mol^{-1}. Only a slow addition of O_2 was observed. However, the reported OA of Ta^+ has a ± 15 kcal mol^{-1} uncertainty associated with it, and our results could be used as an indication that a more accurate value is closer to the lower limit of the reported range.

Other experimental work in our laboratory showed that some early transition metal cations attach more than two molecules of benzene.[12] The reactivity toward O_2 of such higher-order benzene adducts of transition metal cations was not the subject of the present work, but some observations were made during the high-benzene-flow experiments. Ions with the molecular formulas $La(C_6H_6)_3O^+$, $La(C_6H_6)_3O_2^+$, $Y(C_6H_6)_3O_2^+$, and $Zr(C_6H_6)_3O_2^+$ were observed when a high benzene flow was used. The source of such ions could be the reaction of $M(C_6H_6)_3^+$ with O_2, but also the reaction of $M(C_6H_6)_2^+$ first with O_2 and then with C_6H_6, because in all of these cases, $M(C_6H_6)_2^+$ was not completely depleted. The product ions from the reaction of $M(C_6H_6)_2^+$ with O_2 [$M(C_6H_6)_2O^+$ and $M(C_6H_6)_2O_2^+$] could attach one molecule of benzene in the time frame between their formation and the actual ion sampling, thus generating $M(C_6H_6)_2OC_6H_6^+$ and $M(C_6H_6)_2O_2C_6H_6^+$.

Conclusions

The oxidation of transition metal cation−benzene adducts with molecular oxygen is a selective process depending on the position of the metal cation in the periodic table. Benzene adducts of early transition metal cations show a rich chemistry that involves a competition between several (up to five) reaction channels. The overall reactions are fast, approaching the collision limit.

Activation of the molecular oxygen followed by the transfer of an oxygen atom to the metal−benzene adduct is an intrinsic

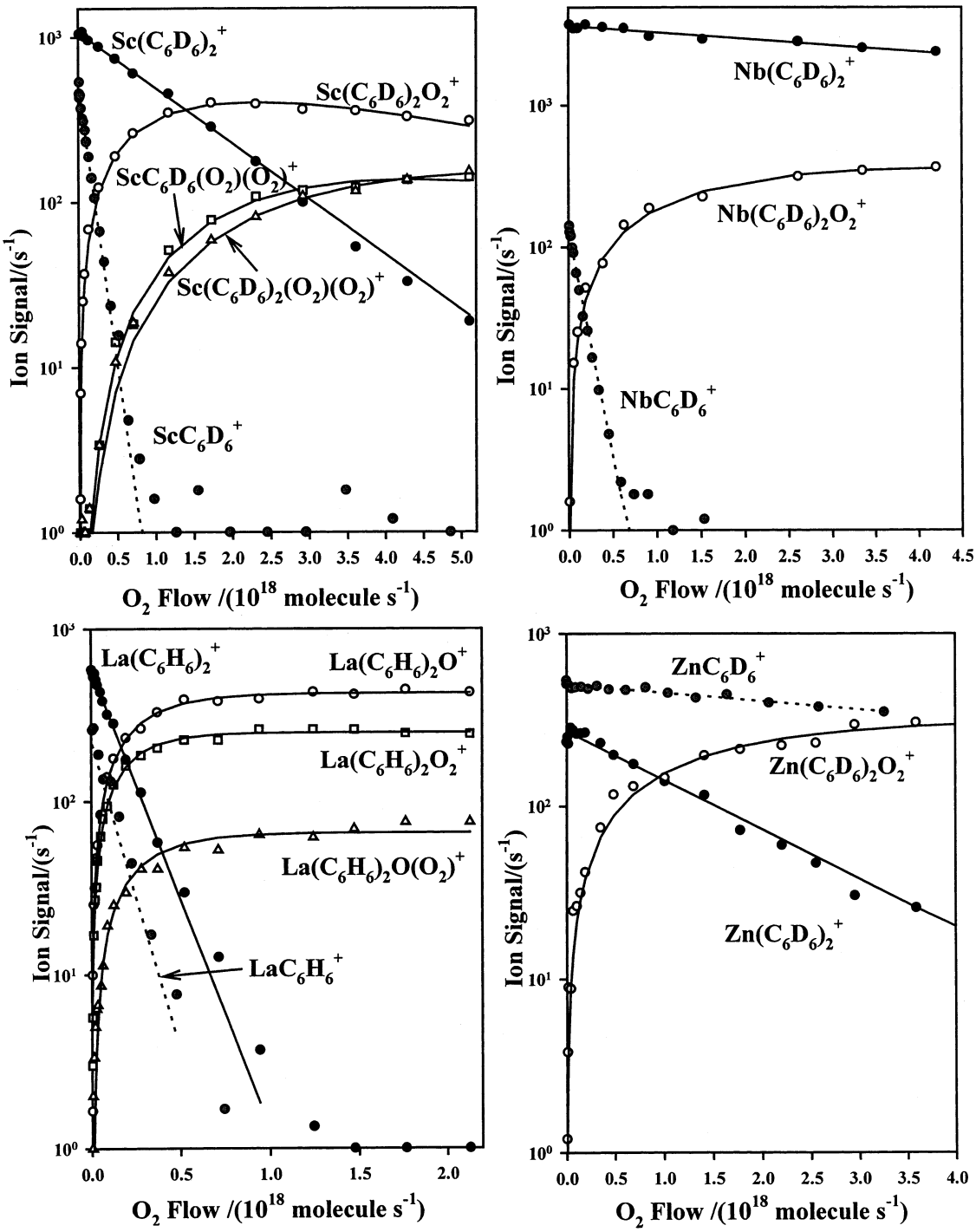

Figure 7. Composite of ICP/SIFT results for the reactions of the selected first-, second-, and third-row transition metal ion−benzene bis-adducts $Sc(C_6D_6)_2^+$, $Nb(C_6D_6)_2^+$, $La(C_6H_6)_2^+$, and $Zn(C_6D_6)_2^+$ with O_2 in helium buffer gas at 0.35 ± 0.01 Torr and 295 ± 2 K. The decays of the corresponding benzene monoadducts monitored in separate (low-flow) experiments are also indicated for comparison.

property of the early metal cations that is preserved in the presence of one benzene ligand and, to some degree, two ligands. Reactions involving switching the benzene ligand with molecular oxygen or abstraction of the metal from the benzene adduct ion result in the formation of cationic or neutral dioxides of early transition metals. The occurrence or nonoccurrence of these channels allows estimations of thermochemical properties of the metal dioxide species to be made. Molecular oxygen addition occurs much faster with metal−benzene adduct ions compared to the bare metal ions and is the exclusive reaction pathway for benzene adducts of late transition metal cations (although no oxygen addition was observed with $AgC_6H_6^+$ and $CdC_6H_6^+$). Rate enhancements of up to 4 orders of magnitude are observed when compared with results obtained in the absence of the benzene ligand.

We have shown that oxidation of the benzene substrate takes place in the presence of metal cations situated at the border between early and late transition metals (Cr^+, Fe^+, Co^+, Re^+). Such reactions result in the formation of ionic or neutral oxygenated benzene species, with or without the metal being retained in their structures. CID experiments were employed to investigate the structures of such ionic species. Catalytic oxidation of benzene takes place in the presence of Cr^+, Fe^+, and Co^+, presumably to form neutral catechol.

Acknowledgment. Continued financial support from the Natural Sciences and Engineering Research Council of Canada is greatly appreciated. Also, we acknowledge support from the National Research Council, the Natural Science and Engineering Research Council, and MDS SCIEX in the form of a Research Partnership grant. As holder of a Canada Research Chair in Physical Chemistry, Diethard K. Bohme thanks the Canada Research Chair Program for its contributions to this research. This work is dedicated to Jack L. Beauchamp on the occasion of his 60th birthday and in recognition of his many outstanding contributions to gas-phase ion chemistry and physical chemistry.

References and Notes

(1) *Organometallic Ion Chemistry*; Freiser, B. S., Ed.; Kluwer Academic Publishers: Dordrecht, The Netherlands, 1996.

(2) (a) Schröder, D.; Schwarz, H.; Shaik, S. *Struct. Bonding* **2000**, *97*, 91−123. (b) Molina-Svendsen, H.; Bojesen, G.; Mckenzie, C. J. *Inorg. Chem.* **1998**, *37*, 1981−1983. (c) Innorta, G.; Torroni, S.; Maranzana, A.; Tonachini, G. *J. Organomet. Chem.* **2001**, *626*, 24−31. (d) Allison, J.; Ridge, D. P. *J. Am. Chem. Soc*. **1977**, *99*, 35. (e) Mandich, M. L.; Steigerwald, M. L.; Reents, W. D. *J. Am. Chem. Soc*. **1986**, *108*, 6197−6202. (f) Wong, P. S.; Ma, S. G.; Cooks, R. G. *Rapid Commun. Mass Spectrom.* **1996**, *10*, 927−931. (g) Bakhtiar, R.; Jacobson, D. B. *J. Am. Soc. Mass Spectrom.* **1996**, *7*, 938−952. (h) Gapeev, A.; Dunbar, R. C. *J. Phys. Chem. A* **2000**, *104*, 4084−4088. (i) Gapeev, A.; Dunbar, R. C. *J. Am. Soc. Mass Spectrom.* **2002**, *13*, 477−484.

(3) (a) Dougherty, D. A. *Science* **1996**, *271*, 163−168. (b) Ma, J. C.; Dougherty, D. A. *Chem. Rev.* **1997**, *97*, 1303−1324. (c) Ryzhov, V.; Dunbar, R. C. *J. Am. Chem. Soc*. **1999**, 121, 2259−2268.

(4) Ho, R. Y. N.; Liebman, J. F.; Valentine, J. S. In *Active Oxygen in Biochemistry*; Blackie Academic & Professional: Glasgow, Scotland, 1992; pp 1−37.

(5) (a) Bohme, D. K. *Chem. Rev*. **1992**, *92*, 1487. (b) Boissel, P. *Astron. Astrophys.* **1994**, *285*, L33. (c) Pirani, F.; Cappelletti, D.; Bartolomei, M.; Aquilanti, V.; Scotoni, M.; Vescovi, M.; Ascenzi, D.; Bassi, D. *Phys. Rev. Lett.* **2001**, *86*, 5035−5038.

(6) Koyanagi, G. K.; Caraiman, D.; Blagojevic, V.; Bohme, D. K. *J. Phys. Chem. A* **2002**, *106*, 4581−4590.

(7) (a) Golding, B. T.; Watson, W. P. *Exocyclic Nucleic Acid Adducts in Carcinogenesis and Mutagenesis*; Singer, B., Bartsch, H., Eds.; International Agency for Research on Cancer: Lyons, France, 1999; Chapter 2, pp 75−88. (b) Medinsky, M. A.; Kenyon, E. M.; Seaton, M. J.; Schlosser, P. M. *Environ. Health Perspect.* **1996**, *Suppl. 6*, 104.

(8) Passoni, L.; Cruz, A.; Buffon, R.; Schuchardt, U. *J. Mol. Catal. A: Chem.* **1997**, *120*, 117−123.

(9) (a) Kappes, M. M.; Staley, R. H. *J. Am. Chem. Soc.* **1981**, *103*, 1286−1287. (b) Sievers, M. R.; Chen, Y. M.; Haynes, C. L.; Armentrout, P. B. *J. Am. Soc. Mass Spectrom.* **1999**, *10* (9), 821−839. (c) Schalley, C. A.; Schröder, D.; Schwarz, H. *Organometallics* **1995**, *14*(1), 316−326.

(10) (a) Mackay, G. I.; Vlachos, G. D.; Bohme, D. K.; Schiff, H. I. *Int. J. Mass Spectrom. Ion Phys.* **1980**, *36*, 259−270. (b) Baranov, V.; Bohme, D. K. *Int. J. Mass Spectrom. Ion Processes* **1995**, *149*/*150*, 543−553.

(11) Koyanagi, G. K.; Lavrov, V. V.; Baranov, V.; Bandura, D.; Tanner, S.; McLaren, J. W.; Bohme, D. K. *Int. J. Mass Spectrom.* **2000**, *194*, L1−L5.

(12) Koyanagi, G. K.; Bohme, D. K. Periodic Trends in the Clustering of Benzene to Metal Cations: Potassium through Bismuth. In *Proceedings of the 50th ASMS Conference on Mass Spectrometry and Allied Topics*; Orlando, Florida, June 2−6, 2002.

(13) Baranov, V.; Bohme, D. K. *Int. J. Mass Spectrom. Ion Processes* **1996**, *154*, 71−88.

(14) Lias, S. G.; Bartmess, J. E.; Liebman, J. F.; Holmes, J. L.; Levin, R. D.; Mallard, W. G. Ion Energetics Data. In *NIST Chemistry WebBook, NIST Standard Reference Database*, Number 69; Mallard, W. G., Linstrom, P. J., Eds.; National Institute of Standards and Technology: Gaithersburg, MD, Feb 2000 (http://webbook.nist.gov).

(15) Su, T.; Chesnavich, J. *J. Chem. Phys.* **1982**, *76*, 5183−5185.

(16) *J. Phys. Chem. Ref. Data* **1988**, *17* (Suppl. 1).

(17) Milburn, R. K.; Baranov, V. I.; Hopkinson, A. C.; Bohme, D. K. *J. Phys. Chem. A* **1998**, *102*, 9803−9810.

(18) Fisher, E. R.; Elkind, J. L.; Clemmer, D. E.; Georgiadis, R.; Loh, S. K.; Aristov, N.; Sunderlin, L. S.; Armentrout, P. B. *J. Chem. Phys.* **1990**, *93*, 2676−2691.

(19) Meyer, F.; Khan, F. A.; Armentrout, P. B. *J. Am. Chem. Soc.* **1995**, *117*, 9740−9748.

(20) Carter, E. A.; Goddard, W. A. *J. Phys. Chem.* **1988**, *92*, 5679−5683.

(21) Armentrout, P. B.; Kickel, B. L. In *Organometallic Ion Chemistry*; Kluwer Academic Publishers: Dordrecht, The Netherlands, 1996; pp 1−45.

(22) Schröder, D.; Zummack, W.; Schwarz, H. *Organometallics* **1993**, *12*, 1079−1085.

(23) Brönstrup, M.; Schröder, D.; Schwarz, H. *Chem. Eur. J.* **2000**, *6*, 91−103.

(24) Lewars, E. *Can. Chem. Rev.* **2000**, *78*, 297−306.

(25) Chase, W. C. NIST−JANAF Themochemical Tables, 4th ed. *J. Phys. Chem. Ref. Data*, *Monograph 9* **1998**, 1−1951.

(26) Martin, W. C.; Musgrove, A. *Ground Levels and Ionization Energies for the Neutral Atoms*; National Institute of Standards and Technology: Gaithersburg, MD, 1999 (http://physics.nist.gov/PhysRefData/IonEnergy).

(27) Bauschlicher, C. W.; Partridge, H.; Langhoff, S. R. *J. Phys. Chem.* **1992**, *96*, 3273−3278.

(28) Schröder, D.; Brown, R.; Schwerdtfeger, P.; Schwarz, H. *Int. J. Mass Spectrom.* **2000**, *203*, 155−163.

(29) Greenberg, A. In *Active Oxygen in Biochemistry*; Blackie Academic & Professional: Glasgow, Scotland, 1992; pp 401−433.

(30) (a) Hallier-Soulier, S.; Ducrocq, V.; Truffaut, N. *Can. J. Microbiol.* **1999**, *45* (11), 898−904. (b) Irie, S.; Doi, S.; Yorifuji, T.; Takagi, M.; Yano, K. *J. Bacteriol*. **1987**, *169* (11), 5174−5179.

(31) Kitano, T.; Kuroda, Y.; Itoh, A.; Jian, L.; Kunai, A.; Sasaki, K. *J. Chem. Soc., Perkin Trans. 2* **1990**, *11*, 1991−1995.

(32) (a) Schröder, D.; Schwarz, H. *Helv. Chim. Acta* **1992**, *75*, 1281−1287. (b) Ryan, M. F.; Stockigt, D.; Schwarz, H. *J. Am. Chem. Soc.* **1994**, *116*, 9565−9570.

(33) Schröder, D.; Schwarz, H. *Angew. Chem., Int. Ed. Engl.* **1993**, *32*, 1420−1422.